78-767

The Induction Driven Tunnel at ONERA-CERT

Roger Michel,* André Mignosi,† and Claude Quemard‡
Office National d'Etudes et de Recherches Aerospatiales (ONERA), Centre d'Etudes et de Recherches de Toulouse (CERT) Toulouse Cedex, France

A new transonic wind tunnel, conceived as a pilot unit by ONERA for the large European high Reynolds number tunnel project, has been operating since 1975 at the ONERA research center in Toulouse. After a brief overview of the main characteristics of this wind tunnel T2, a description is given of the testing techniques which have been developed for studies of flow around models. Two examples of applications are concerned with the definition of viscous and nonviscous flows over an aerofoil and over a tapered swept-wing model. Pressure measurements, wall flow vizualizations, and probing of boundary layers and wakes bring detailed elements for assessing calculation methods involving a coupling between viscous and potential flows.

I. Introduction

THE T2 transonic wind tunnel, conceived as a pilot unit by ONERA for their project of a Large European High Reynolds Number Tunnel (LEHRT) has been operating since 1975 at the ONERA Research Center in Toulouse. Three projects were developed: 1) the Ludwieg tube from DFVLR, Germany,[1] 2) the Evans clean tunnel from RAE, Great Britain,[2] and 3) the pressurized injector driven (IDT) from ONERA, France. The wind tunnel is the 0.1 scale model of that third project.

Within the qualification tests required for the three project pilot units, the implementation of the T2 wind tunnel was subject to elaborate studies. One of the main goals was to optimize the drive system and especially to prove that the flow quality of an IDT can be satisfactory despite a high aerodynamic noise which can be produced by the driving jets.

After a brief review of the wind-tunnel main operating characteristics and of the solutions proposed to reduce the flow variations in the test section, we shall present a few examples showing that the flow quality fulfils the very strict requirements set for the LEHRT transonic wind tunnel project for short flow duration. The second part of the paper deals with the wind-tunnel use as a research unit in order to study subsonic and transonic flows in detail. To that effect, the wind tunnel has been equipped with various measurement devices which enabled detailed knowledge of the viscous and nonviscous flows around models. We shall present and analyze a set of typical results obtained during two series of systematic tests. The first series concerned a thick wing profile (NACA 65217). With the boundary layers and wake development, we obtained some detailed experimental assessment information for calculation methods of subsonic and transonic flowfields.

To set forth the problems from a rather general point of view, we decided to study a tapered swept-back wing model mounted on a half-fuselage at the test section wall. The implementation of the various experimental techniques allowed us to obtain a detailed description underlining the flow three-dimensionality aspects.

II. The Wind-Tunnel Main Characteristics

Special care has been taken in the design of the T2 wind tunnel as well as in some of the improvements specially meant to obtain low levels of pressure and velocity fluctuations in the test section. As the detailed description and performance of the wind tunnel were the object of previous publications,[3,4] only its main characteristics will be recalled.

T2 is a transonic injector driven tunnel in which Mach numbers up to 1.1 can be reached in a 40×40-cm test section; the running time is approximately 30 s at maximum mass flow. A general layout of the aerodynamic circuit and air supply facilities is schematized in Fig. 1. The diagram in Fig. 2 shows that a Reynolds number of 7.5 million can be reached at the nominal Mach number, $M=0.9$, with a 10-cm-chord model.

A characteristic aspect of T2 is that the driving fluid injection is provided through the trailing edges of the vanes of the first corner after the test section; so the injection involves 7 jets which rapidly mix with the induced flow. The emission of jet noise is located far from the test section and essentially directed towards the return duct, this being propitious to a damping of acoustic energy.

In order to optimize the performance and the flow quality, it appears very important to provide for a variation of the injector exit to mixing cross-section area ratio λ; the selected solution is to partition the inside of each vane so as to form 14 small nozzles giving the required Mach number $M_j=1.6$ and supplied with compressed air by groups of 6 and 8 (Fig. 3).

Another typical aspect of T2 is that the flow removal is located just upstream of the injector; taking advantage of the pressure level in the wind tunnel, it is simply performed through the porous walls of a rectangular cross-section duct, acting as a diffuser after the test section. The advantages of such a solution are obvious. First, the suction of the wall boundary layer reduces the total pressure losses of the circuit. Second, the injector has to drive only the difference between the mass flow in the test section and the removed mass flow.

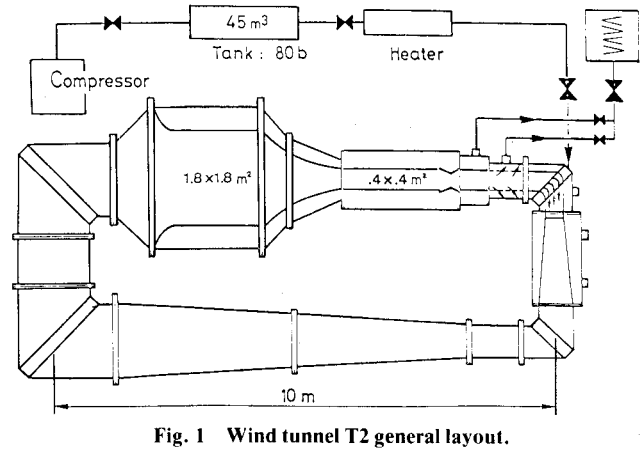

Fig. 1 Wind tunnel T2 general layout.

Presented as Paper 78-767 at the AIAA 10th Aerodynamic Testing Conference, San Diego, Calif., April 19-21, 1978; submitted June 1, 1978; revision received Sept. 12, 1978.

Index category: Transonic Flow.

*Head of Aerothermodynamics Dept.
†Research Engineer.
‡Head of Research Group.

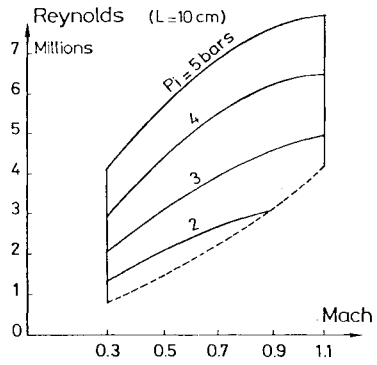

Fig. 2 T2 performance.

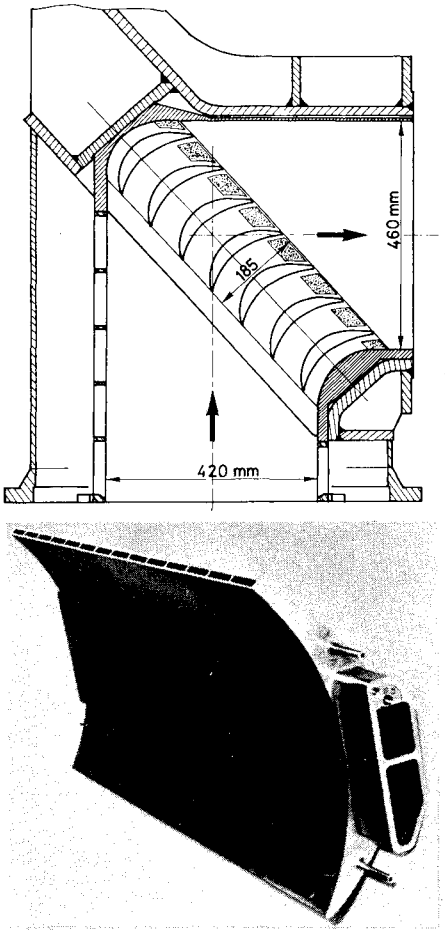

Fig. 3 T2 injector corner system.

Finally, let us say that the upper and lower walls of the test section can diverge, or converge, for the adjustment of the Mach number uniformity. In the tests presented later, the walls are solid, with an angle of divergence of 0.35 deg; they can also be porous, the test section communicating with the upper and lower parts of the plenum chamber.

Using the high-performance data acquisition system presented further on, and within the qualification test requirements for pilot units for the European project,[5] we were led to make a thorough analysis of the flow fluctuations. The LEHRT PG.7 Working Group defined large bandwith probes and transducers (up to 40 kHz) in order to determine velocity, pressure, Mach number, and flow direction fluctuations in the three candidate tunnels. In fact, such a tool helped us develop measurement techniques now currently used in T2 and described further on.

By means of a carefully shaped second throat at the rear of the test section, and by an optimization of the area ratio and of the configuration of the jet nozzles, it was possible to

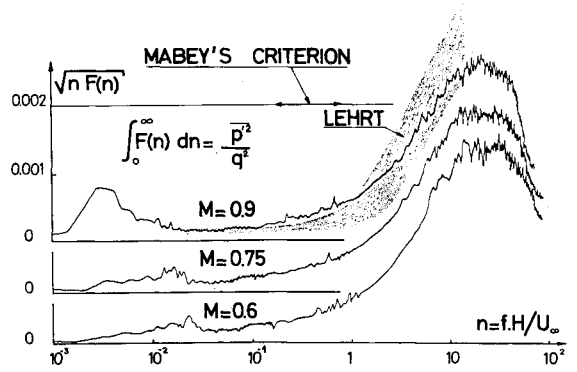

Fig. 4 Pressure fluctuations spectra in test section.

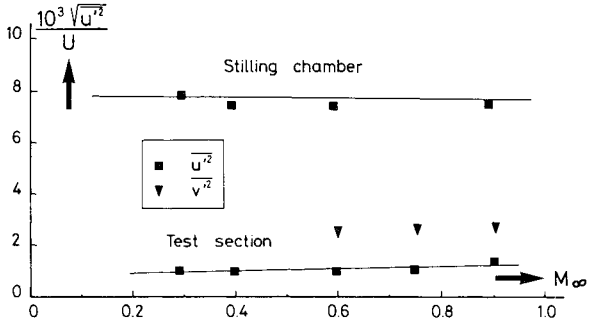

Fig. 5 rms velocity fluctuations.

reduce considerably the fluctuations, and obtain results exemplified in Figs. 4 and 5.

We show in Fig. 4 the pressure fluctuation spectra measured at the test section wall. They are given with the conventional coordinates, n being the reduced frequency fh/U_∞ (h being the height of the test section, U_∞ the velocity), and $F(n)$ the reduced energy defined by

$$\int_{\text{band}} F(n)\,dn = \frac{\overline{P'^2}}{q^2}, \quad q = \frac{1}{2}\rho_\infty U_\infty^2$$

At high frequencies, the noticeable fluctuation increase obviously arises from the boundary-layer noise. The level remains low up to a reduced frequency $n = 1$, that is in the frequency range where the flow fluctuations may have an effect on the main phenomena to be studied in transonic aerodynamics.

Figure 5 shows the intensity of longitudinal (u') and transverse (v') components of velocity fluctuation. As previously described, the reduced fluctuations, quite independent from Mach number, remains at low levels (in the order of 10^{-3}). Qualities obtained for the flow then appear compatible with the European transonic wind-tunnel requirements.[6] We stress the strictness of these requirements, which were expressed a priori for short flow duration facilities. The required level is really more stringent than Mabey's criterion, which is often used for normal wind tunnels.[7] The efforts made toward this goal allowed us to obtain quite exceptional flow qualities in T2.

III. Data Acquisition and Measurements Techniques

Data Acquisition System

The T2 wind tunnel is fitted with a data acquisition system based upon a Hewlett-Packard 2100 A computer with 16-k words memory. The 16 analog channels are composed of amplifiers-conditioners, followed by filters for selecting the frequency range used. They are sampled at a high rate by an analog-digital multiplex converter. Information is recorded

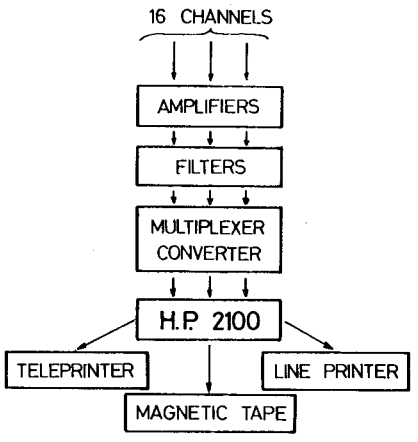

Fig. 6 Data acquisition system.

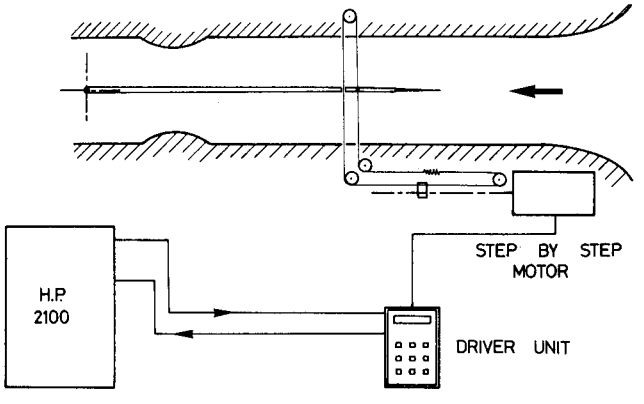

Fig. 7 Experimental system for boundary layers and wake.

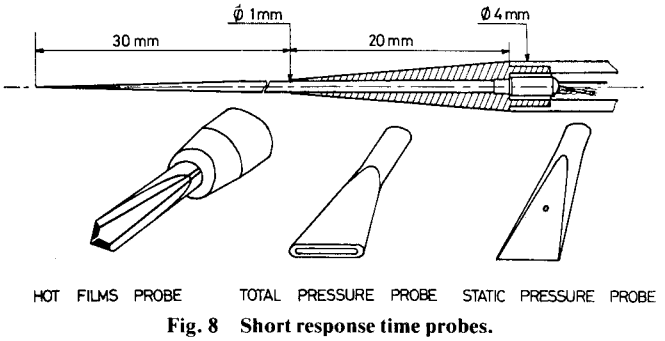

Fig. 8 Short response time probes.

on a digital magnetic tape. A teleprinter and line printer complete the system (Fig. 6). The rates allowed by the multiplex converter give, according to the number of channels, the usable bandwidths – from 40 kHz with one channel, it proportionally decreases to 5 kHz with eight channels in use.

When the simultaneous acquisition of several parameters in a large bandwidth is required, we first record the data on an analog magnetic tape recorder and convert them after the run. Presently, the data reduction is achieved off-line with the CERT-IRIS 80 computer. Results are available both as listings and Benson drawings.

Measurement Devices

Besides the usual mean pressure measurements via a scanivalve, our aim was to define means of studying boundary layers and wakes. The complete surveying system is shown on Fig. 7. It is mainly composed of a conical mast, parallel to the test section centerline, with a rotation point located downstream of the second throat; the end is pulled in a vertical

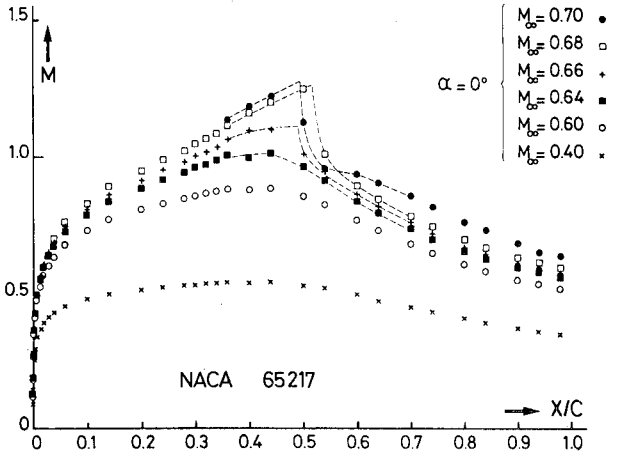

Fig. 9 Local Mach number distributions on 65217 profile.

plane by a cable moved by a step-by-step motor; the computer monitors the moving rate and the rest duration for each measuring point. One can move the whole system to probe the boundary or the wake at different spanwise locations. The mast can be fitted with pressure probes and hot film probes.

Pressure probes (Fig. 8) are made from small diameter ($\phi = 1$ mm) pipes; the tip of the total pressure probe is flattened to about 0.1-mm thickness. They are lengthened with a 4-mm-diam pipe in which is put a 1.3-mm-diam Kulite XCOL transducer and its thermal compensation.

A static pressure probe has been achieved according to the same rules, with a 0.8-mm-diam transducer. The maximum diameter of the probe is now reduced down to 2 mm and the small volume between the pressure holes and the transducer allows a several-kHz bandwidth.

In the steady flow experiments presented later, the bandwidth was a few tens of Hz. The advantage of such a probe design is of course the short response time which allows a fast enough translation to explore a boundary layer with a good accuracy in a single 30- to 60-s run. The data acquisition system simultaneously operates at a rate of about 200 points/s, and each measurement is finally the average of a few tens of instantaneous values.

Disa hot film probes R72 have been used to measure the velocity fluctuations and the flow directions. They have diamond-shaped tips, with a small leading-edge radius; such a shape is required for significant measurements in transonic regime. With two hot films put on each face of the diamond, the signal differences allows, after calibration, the determination of the flow direction.

IV. Examples of Results

The measurement techniques just described have been applied both to the study of a wing profile and a swept-wing model. A few characteristic results for these two series of systematic experiments are given in the following.

Study of a Wing Profile

The aim of this study, which was made on a NACA 65217 profile with 12-cm chord, was to bring to light the various aerodynamic experimental results which can represent a detailed assessment of theoretical methods for the coupling between potential and viscous flows.

Pressure Measurements

First, we had to define the potential flow around the profile, i.e., measuring, by means of 70 pressure taps placed in the central section, the distribution of surface pressures. An example of these results is given in Fig. 9 with local Mach number distribution at zero incidence on the upper surface.

After some subsonic-type distributions, a spreading of a supersonic area is observed, ended with a rapid recompression

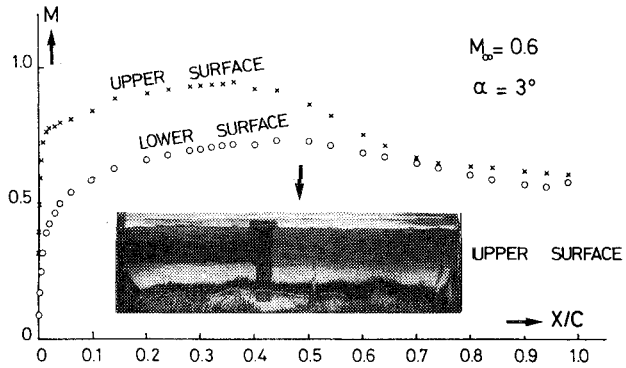

Fig. 10 Local Mach numbers and wall-flow visualization.

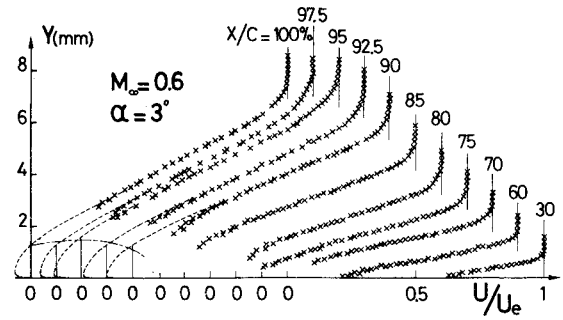

Fig. 11 Boundary-layer profiles on the upper surface.

corresponding to a shock wave. In this case, it is also observed that this shock wave ceases to move back toward the trailing edge from $M_\infty = 0.68$; this phenomenon is probably due to a boundary-layer separation induced by the shock wave.

Surface Flow Visualizations

We also implemented, particularly for finding the separation locations, a visualization technique consisting in covering the surface with an oil and lampblack mixture. Figure 10 gives an example of such a visualization for the profile upper surface with an incidence of 3-deg, $M = 0.6$; the mixture is carried along to areas where the wall friction is rather large; these are white on the photograph. The mixture remains in place in areas where the wall friction is small and they are black on the photograph.

In the case we studied, the transition was promoted by a roughness band, just after the leading edge. The visualization shows clearly that a turbulent separation appears at about 70% on the chord; an almost constant pressure is also established on the rear part.

Study of the Boundary Layers and Wake

It is for the previous configuration that we present, as an example, the detailed results we obtained during the experimental study of the profile boundary layer and wake. The boundary-layer velocity profiles measured on the upper surface are shown on Fig. 11.

Although the boundary-layer thickness is very small, it can be seen that a well-defined turbulent profile is obtained at the first station. Then the boundary layer develops rapidly and the profiles show an almost linear aspect from 75% chord, typical of a separation occurrence which extends afterwards up the trailing edge.

Of course, the total pressure probe used does not permit a measure of the velocities in the near-wall return flow. To obtain the integral characteristics (displacement and momentum thickness) we had to extrapolate the profiles to the wall. For that, we used a wake profile

$$\frac{u-u_c}{u_e-u_c} = \sin^2\left(\frac{\pi y}{2\delta}\right)$$

which should almost correctly represent the separated profiles, provided that a slip velocity at the wall u_c is well chosen.[8] Before analyzing the velocity profiles in the wake, it is useful to consider the pressure distribution downstream of the profile, measured with the static probe of Fig. 8. Their evolution is quite sophisticated (Fig. 12). Thanks to probings restrained at the trailing edge, it is first observed that, as a whole, the static pressure increases until $x/c = 1.10$, meaning that the recompression observed on the rear part of the profile still goes on after the trailing edge.

So, the static pressure jump from one side of the trailing-edge axis to the other does extend the difference between pressures measured at the profile upper and lower surfaces. This characteristic, related to the upper surface separation, damps down quickly and finally disappears between $x/c = 1.05$ and 1.10.

After $x/c = 1.05$, static pressures have a gradient, the sign of which inverses on the axis. This corresponds with a symmetrical curvature of the streamlines on each side of the wake mean line. At $x/c = 1.4$, the curvature is small and the static pressure has almost reached the upstream freestream pressure.

The total pressure profiles are measured in the wake and the same probe as for the boundary layer is used; the velocity profiles are shown in Fig. 13. Due to the high static pressure variation, it is essential to calculate the u velocity in the wake by using the local pressure; u is divided by u_p, a "local potential velocity" calculated from the local static pressure and the potential flow total pressure.

It is interesting to note the quick increase of the minimal velocity, equaling half the velocity u_p at $x/c = 1.10$. At the same time, the profiles quickly tend to become symmetrical. This is interesting, mainly because it becomes possible to envisage practical methods for calculating the wakes, using asymptotic profiles, in the theoretical study of the coupling between potential and viscous flows.

Application and Assessment of Calculation Methods

It is particularly important, for the kind of studies performed, to develop, in parallel with experimental research, calculation methods for the nonviscous and viscous flows, in order to obtain a reciprocal control of these two essential tools. In this regard, for the potential flow, we applied a calculation program using the transonic small perturbation assumptions, established at ONERA by Chattot.[9] This method offers the advantage of taking into account the wall influence.

Calculation programs for turbulent boundary layers were established at the Toulouse Research Center Aerothermodynamic Department[10,11] and are currently used for practical problems under the form of integral methods. Similarly, we deal with the two-dimensional wakes by means of an integral method using the velocity profiles properties which are obtained by turbulent asymptotic similarity solutions. Finally, a simple coupling method consists in adding the displacement thickness to the profile, then introduces sources in the wake, the intensity of which is tied up to the displacement thickness rate of growth. It is then possible to calculate the complete flowfield around a profile, taking into account the test section walls.

Adjustments are still necessary when dealing with sophisticated problems of strong shock-boundary-layer interaction or large separation. We shall only compare the calculation results with those from experiments relative to subcritical domain, without boundary-layer seapration, by considering the flow at $M = 0.6$ for the 65217 profile at zero incidence (Fig. 14).

We can ascertain that the wall pressure distributions are correctly foreseen and the figure shows that pressure evolution is well represented at the profile rear. A good

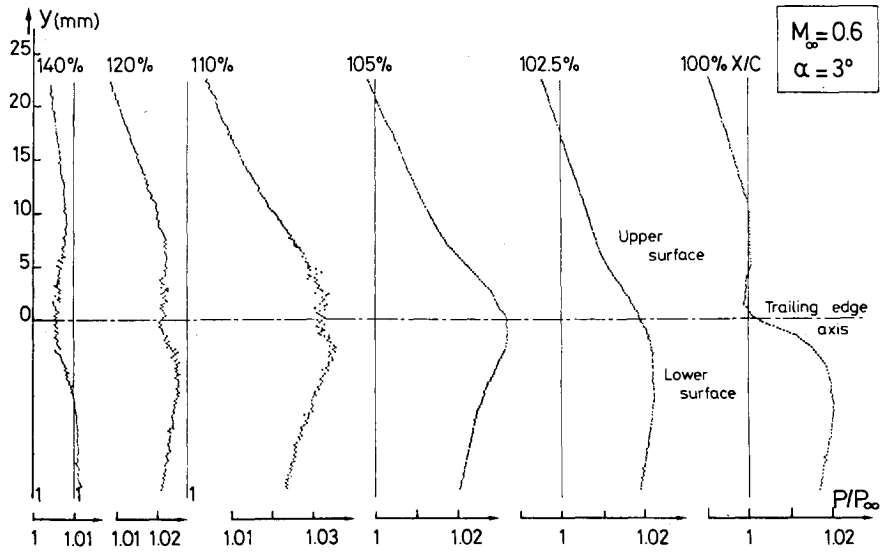

Fig. 12 Static pressure distributions in the wake.

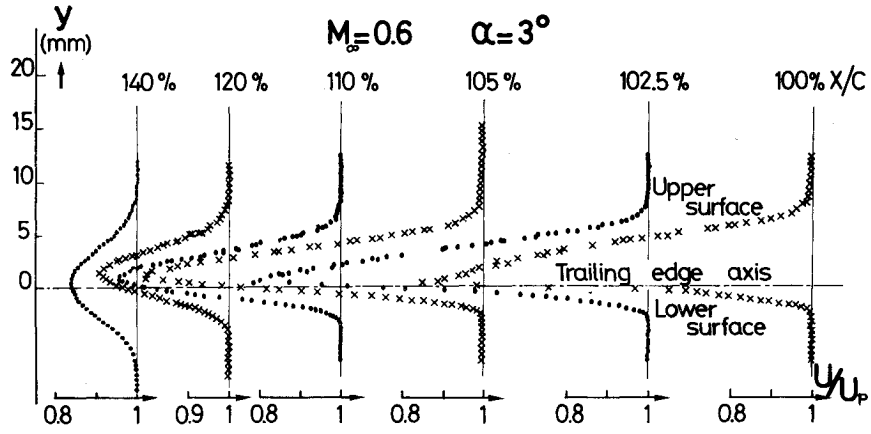

Fig. 13 Velocity profiles in the wake.

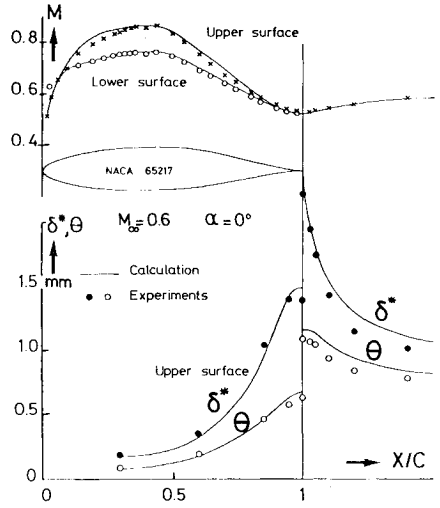

Fig. 14 Comparison with a complete coupling method of calculation.

agreement is also obtained in fact for the static pressure vertical distributions in the wake. Furthermore, the boundary layers at the upper and lower surface have displacement and momentum thickness in good agreement with the measured values.

Study of a Swept Wing Model

This study, whose aim is to emphasize the three-dimensional aspects of the experimental analyses which can be effected in T2 wind tunnel, is made on a swept-wing model, mounted on a half-fuselage at the test section lateral wall; the wing span is 31 cm.

Pressure Distributions

Pressures are measured in five sections along the span (whose positions are shown on one of the visualization photographs, Fig. 15). The study covers a range from $M=0.470$ to $M=0.833$ for incidences included between -2 to $+1$ deg. Results at $M=0.833$ and $M=0.470$ at zero incidence are presented as examples on Fig. 16.

In the supercritical case $M=0.833$, we observe two shocks at the upper surface, particularly obvious in sections 1, 2, and 3. The lower surface shock wave follows a line situated at about 50% of the local chord. The subcritical case ($M=0.470$) is the one for which we shall present the study of the boundary layers and wakes. It appears that the pressure distributions vary only slightly from one wing section to the other. In particular at the upper surface, an almost uniform pressure is observed on the main part of the wing, which explains the small deviations of the wall streamlines before the trailing edge.

Wall Flow Visualizations

Even more than for a profile study, this technique gives valuable information on the boundary-layer development at the lower and upper surface of a wing. Figure 15 shows the visualizations at $M=0.470$ and $\alpha=0$ deg. At the upper surface, a high-velocity peak is followed by a separation bubble after which the boundary layer becomes turbulent; the wall streamlines diverge only slightly in the quasiuniform

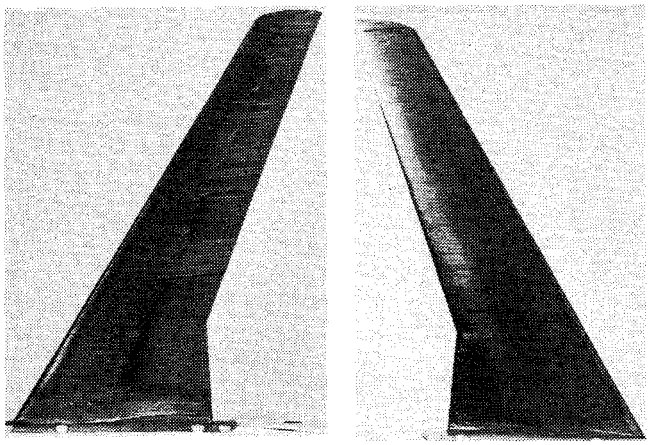

a) lower surface b) upper surface

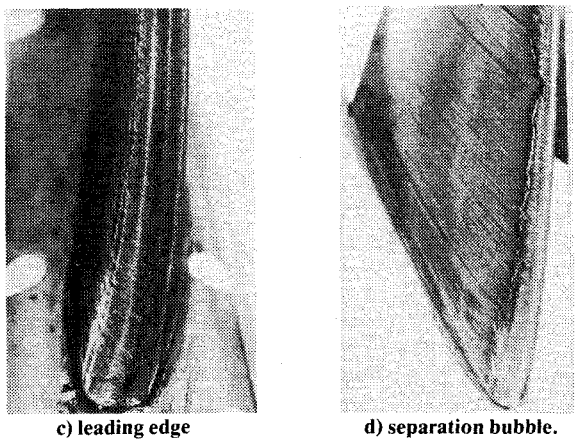

c) leading edge d) separation bubble.

Fig. 15 Wall-flow visualizations ($M=0.47$, $\alpha=0$ deg).

pressure field; then they turn sharply near the trailing edge to become perceptibly parallel to it.

At the lower surface, the boundary layer submitted to an accelerated external flow remains laminar until about half of the chord. As soon as the pressure gradient changes sign, a three-dimensional laminar separation is observed, well shown by a sharp deviation of the wall streamlines, which become nearly parallel to the leading edge. The boundary layer reattaches in turbulent flow; then the wall streamlines remain again parallel to the direction of the upstream velocity.

Study of the Boundary Layers and Wake

Due to the small deviations recorded on the wing, we have been able to define the boundary layers which develop at the upper and lower surfaces, by means of total pressure profiles using a single probe, as in the wing profile case. We analyzed, more particularly, the three-dimensional aspects which occurred near the wing trailing edge and downstream in the wake. We used the double hot film probe technique to determine the velocity and flow direction profiles.

Figure 17 gives the lateral direction angle profiles, measured at the trailing edge, at a half-chord and at one chord downstream. The main observation concerns the rapid decrease of the deviation angle when moving away from the trailing edge.

Although they are preliminary, these results show the promise of hot film probes for the study of three-dimensional subsonic and transonic flows; this technique can be improved both with higher sampling rates giving a better definition of the mean values and the use of smaller probes.

V. Conclusions

A brief review of the main characteristics of the induction T2 wind tunnel allowed us to underline the rather exceptional

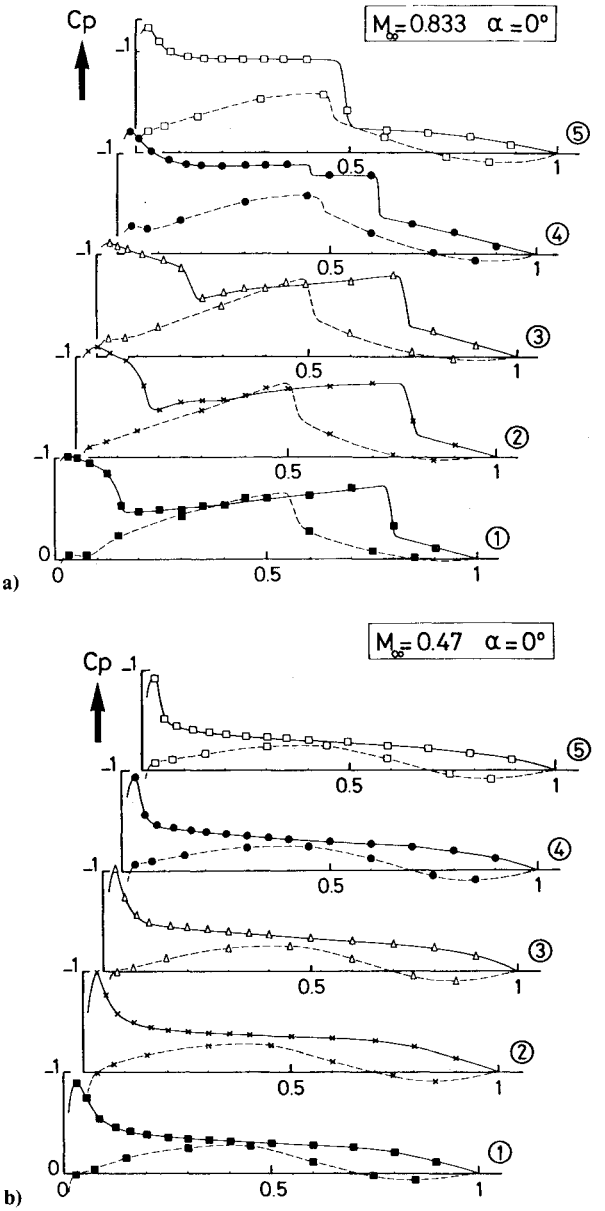

Fig. 16 Pressure distributions along the span for the swept-wing model.

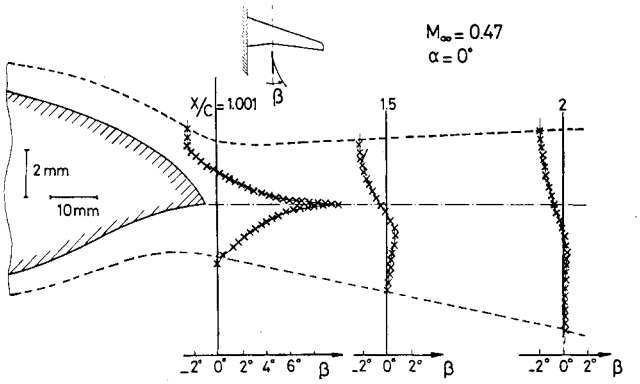

Fig. 17 Transverse flow profiles at trailing edge and in the wake.

qualities of the flow, with the very low fluctuation levels which are recorded for pressure and velocity in the test section. The wind tunnel is equipped with a digital data acquisition system allowing systematic tests with a good rate of runs. Special efforts have also been made to obtain devices allowing a detailed definition of the flow around the models.

Two applications examples of these techniques concerned the study of a wing profile and of a tapered swept wing. The aforementioned results, presented here to show the possibilities offered by the wind tunnel, allow us to point out and specify the essential characteristics of the subsonic-transonic flow around models. We consider that the wind tunnel is now operational for elaborate studies which will give the necessary elements for a comparison of theories and calculation methods for viscous and nonviscous flows.

References

[1]Ludwieg, H., Grauer-Carstensen, H., and Lorenz-Meyer, W., "The Ludwieg Tube. A Proposal for a High Reynolds Number Transonic Wind-Tunnel," *AGARD Conference Proceedings on Wind Tunnel Design and Testing Techniques,* No. 174, 1976.

[2]Pugh, P.G., Beckett, W.A., and Gell, T.G., "The E.C.T. Drive System: A Demonstration of Its Practicability and Utility," *AGARD Conference Proceedings on Wind Tunnel Design and Testing Techniques,* No. 174, 1976.

[3]Michel, R., Quemard, C., and Mignosi, A., "Problemes Liés à la Définition et à la Mise au Point d'une Soufflerie Transsonique Pressurisée à Induction," *AGARD Conference Procedings,* No. 174, 1976.

[4]Quémard, C. and Mignosi, A., "Definition of a High Flow Quality Injector Driven Tunnel: the Pressurized Transonic Wind Tunnel T2 of ONERA/CERT," *18th Israel Annual Conference on Aviation and Astronautics,* ONERA TP 1976-52, Haifa, May 19-21, 1976.

[5]Pugh, P.G., Grauer-Carstenson, H. and Quémard, C., "An Investigation of the Quality of the Flow Generated by Three Types of Pilot Wind-Tunnel (Ludwieg Tube, Evans Clean Tunnel and Injector Driven Tunnel)," AGARD-R-, proposed synopsis AGARD memorial, to be published.

[6]Hartzuiker, J.P., Pugh, P.G., Lorenz-Meyer, W., and Fasso, G.E., "On the Flow Quality Necessary for the Large European High Reynolds Number Transonic Wind-Tunnel LEHRT," AGARD-R-644, 1976.

[7]Mabbey, D.G., "The Influence of Flow Unsteadiness on Wind-Tunnel Measurements at Transonic Speeds," Royal Aircraft Establishment, Tech. Memo Aero 1473, 1973.

[8]Carrière, P., Sirieix, M., and Delery, J., "Méthode de Calcul des Écoulements Turbulents Décollés en Supersonique," *Progress in Aerospace Sciences,* Vol. 16, 1975, pp. 385-429.

[9]Chattot, J.J., "Écoulements Transonniques avec Chocs. Méthode de Murman-Cole-Krapp pour l'Équation Transsonique des Pétites Perturbations," ONERA, Document intérieur, 1973.

[10]Michel, R., Quémard, C., and Cousteix, J., "Méthode Pratique de Prévision des Couches Limites Turbulentes en Bi et Tridimensionnel," ONERA, Recherche Aerospatiale, No. 1972-1.

[11]Cousteix, J., "Progres dans les Méthodes de Calcul des Couches Limites Turbulentes Bi et Tridimensionnelles," ONERA Note Technique, No. 1976-15.